

Chapter 1

Introduction

In the working environment, a human in drowsiness often exhibits relative inattention to environments, eye closure, less mobility, failure to motor control and decision making [1]. Therefore, many disasters and near-disasters can be caused by falling drowsiness especially for machine operators who pose a danger not only to themselves but often also to the public at large. Recently, safety driving has received increasing attention of the public due to the growing number of traffic accidents.

Drivers' fatigue has been implicated as a causal factor in many traffic accidents. The National Sleep Foundation (NSF) reported that 60% of adult drivers (about 168 million people) felt drowsy while driving vehicles and 37% or 103 million people actually fell asleep during driving in 2005. Additionally, the sleep related crashes are most common in young people, especially for adult males and shift workers [2]. NSF also reported that adults aged between 18-29 years old are much more likely to drive while drowsy compared to other age groups. Males are more likely than females to drive while drowsy (56% vs. 45%) and males are almost twice as likely as females to fall asleep while driving (22% vs. 12%) investigated in 2002 [2]. Hence, drowsiness detection and prevention is very important to avoid disasters such as vehicle crashes in working environments.

1.1 Current researches of drowsiness

Drivers' fatigue is one of the primary causal factors for many road accidents and hence detection of drowsiness of drivers in real time can help preventing many accidents behind the steering wheel. In the field of safety driving, thus development of methodologies for detection drowsiness / departure from alertness in drivers has become an important area of research. Drowsiness leads to decline in drivers' abilities of perception, recognition, and vehicle control and hence monitoring of drowsiness in drivers is very important to avoid road accidents. It is known that various physiological factors co-vary with drowsiness levels [3–7]. Some such factors are eye activities, heart rate variability (HRV), and the electroencephalogram (EEG) activities. Since the effect of changes in cognitive state on EEG is quite strong, in this study we use EEG as our information source for detection of drowsiness. Most of the earlier studies using EEG relating to assessment of changes in cognitive states are supervised in nature and have used the same detection model for all subjects [8-10]. But it is known that there existed relatively large subjective variability in EEG dynamics relating to drowsiness / departure from alertness. This suggests that for many operators, group statistics or a global model may not be effective to accurately predict changes in the cognitive states [11-14]. Subject-dependent models have also been developed to account for individual variability. Such personalized models

although can alleviate the problem of individual variability in EEG spectra; such methods cannot take into account the variability between sessions in EEG spectra due to various factors such as electrode displacements, environmental noises, skin-electrode impedance, and base-line EEG differences. One of the major problems in dealing with EEG signals in a real time driving environment is the presence of noise. Often independent component analysis (ICA) [15-19] is used for cleaning noise from EEG. However, selection of the noisy components in an automatic manner using ICA is still a difficult task.

1.2. Kinesthetic perception during driving

The driving motion is one of the most experienced kinesthetic perceptions in our life, in other words, the perception we sense during the vehicle speed or direction change.

Whenever the vehicle accelerates, decelerates or curves in a corner, we experience a force pulling our body against the direction of moving. For a driver, the perception of motion includes kinesthetic and visual stimulus. A driver does not sense only the pushing or pulling of his/her body by a force, but also the scene change related to vehicle movement. The driving perception includes the co-stimulation of visual cue, vestibular stimulation, muscle reaction and skin pressure. It is indeed a complicated mechanism to understand.

There are numbers of difficulties in investigating the driving perception. First of all, the safety of subject must be guaranteed. Experiments should be held under a safe driving environment, it is very dangerous to conduct driving experiments on the road. Second, appropriate monitoring and data acquisition are needed to study the influence of kinesthetic stimuli. The stimulation should be simple enough and repeatable to keep experiment under control. Third, objective evaluation should be assessed in the studies.

One of the solutions is to conduct driving experiments using a realistic simulator, which is widely used in driving related researches [20]. For the necessity of motion during driving, literatures showed that the absence of motion information increased reaction times to external movement perturbations [21], and decreased safety margins in the control of lateral acceleration in curve driving [22]. In real driving, improper signals from disordered vestibular organs were reported to determine inappropriate steering adjustment [23]. Moreover, the presence of vestibular information in driving simulators shows the importance for it influences the perception of illusory self-tilt and illusory self-motion [24]. All the above studies emphasized the importance of motion perception during driving with the assessment of driving performance and behavior. Our previous studies also demonstrated that multiple cortical EEG sources

responded to driving events differentially in dynamic and static environment. Specifically, the alpha band variations occurred in many components (Mu, parietal and occipital) during driving, especially when the vehicle is moving. It is still unclear to what extent the kinesthetic stimulation would interfere with the fluctuations of driver's global level of drowsiness accompanying changes in driver's performance.

1.3. Virtual reality dynamic simulator

Virtual reality (VR) technology is gradually being recognized as a useful tool for the study and assessment of normal and abnormal brain function, as well as for cognitive rehabilitation. Virtual Environments (VE) are created by powerful computers that generate realistic animated graphics in three dimensions. Creating carefully controlled, dynamic, 3D stimulus environments combined with physiological and behavioral response recording can be offer more assessment options that are not available by traditional neuropsychological methods.

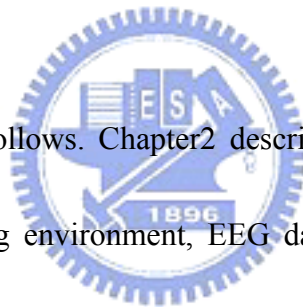
The VR technique allows subjects to interact directly with a virtual environment rather than monotonous auditory and visual stimuli. It is an excellent strategy for brain research on interactive and realistic tasks due to low cost and avoiding risk of operating on the actual machines. In recent years, some researchers designed the VR

senses to provide the appropriate environments for brain activity study [25-27]. Integrating the VR scene with dynamic motion platform is excellent for studying the influence of kinesthetic stimulus on cognitive state. Therefore, a VR-based dynamic motion platform combined with EEG measured system is an innovation in brain and cognitive engineering researches.

1.4 Organization of this thesis

In this investigation we introduce an unsupervised approach to estimate a model for the alert state of the subject. We shall refer to such models as alert-models. A part of this investigation has been reported in [28]. The proposed approach can account for the variability in EEG signals between individuals and between sessions with the same individual. This being an unsupervised approach we do not need a teacher or a labeled training data set with information on whether the driver is in a alert state or drowsy state at every time instant. In this approach, we derive models of the alert state of the subject as characterized by the EEG signal collected during the first few minutes of recording. We assume that during the first few minutes of driving, the driver (subject) will be in an alert state, although he/she may not be in a completely normal state as he/she might have walked some distance to reach the garage. This approach can account for baseline shifts and the variations in EEG spectra due to

changes in recording conditions in different driving sessions. We find that the EEG log power in the alpha band (as well as in the theta band) and the driving performance exhibit a rough linear relation suggesting that changes in the cognitive state is reflected in the EEG power in the two specified bands. We then demonstrate that deviation of the EEG power from that of the alert model also follows a similar relation with the changes in driving performance, and hence with the changes in cognitive state. Consequently, a derivation from the alert model can be used to detect drowsiness and that is what we do in this investigation.



This thesis is organized as follows. Chapter2 describes the EEG-based drowsiness experiment, VR-based driving environment, EEG data collection, instructions, and subjects in the experiments. Chapter3 shows the EEG analysis procedure including behavior analysis, spectra analysis, building alert model, and analyzing the deviation from alert model. Chapter4 shows the experimental results and the discussion is given in chapter5. Finally, we conclude our findings in chapter6.

Chapter 2

System architecture and experimental design

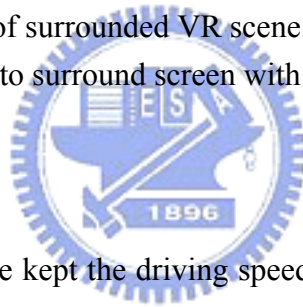
In this study, a VR-based driving system was applied for interactive driving experiment [28]. It included two major parts as shown in (1) the 3D highway driving scene based on the virtual reality technology and (2) the EEG physiological signal measurement system with 32-channel EEG sensors. The full details of experimental system architecture will describe as follows.

2.1 3D virtual reality driving simulation environment

In this study we use a virtual-reality based highway-driving environment to generate the required data. Some of our previous studies to investigate changes in drivers' cognitive states during a long-term monotonous driving have also used the same VR-based environment [29-30]. In this system, a real car mounted on a 6-degree-of-freedom Stewart platform is used for the driving and seven projectors are used to generate 3-D surrounded scenes. During the driving experiments, all scenes move according to the displacement of the car and the subject's maneuvering of the wheels which make the subject feel like driving the car on a real road. The VR environment is showing in Figure 1.



Figure 1. The overview of surrounded VR scene. The VR-based highway scenes are projected into surround screen with seven projectors.



In all our experiments we have kept the driving speed fixed at 100 km/hr and system automatically and randomly drifts the car away from the center of the cruising lane to mimic the effects of a non ideal road surface. The driver is asked to maintain the car along the center of the cruising lane. All subjects involved in this study have good driving skill and hence when the subject is alert, his/her response time to the random drift is short and the deviation of the car from the center of the lane is small. But, when the subject is not alert/ drowsy, both the response time and the car's deviation are high. Note that, in all our experiments, the subject's car is the only car cruising on the VR-based freeway. Although, both response time and the deviation from the

central line are related to the subject's driving performance, in this study, we use the car's deviation from the central line as a measure of performance of the subjects. The driving task is showing in Figure 2.

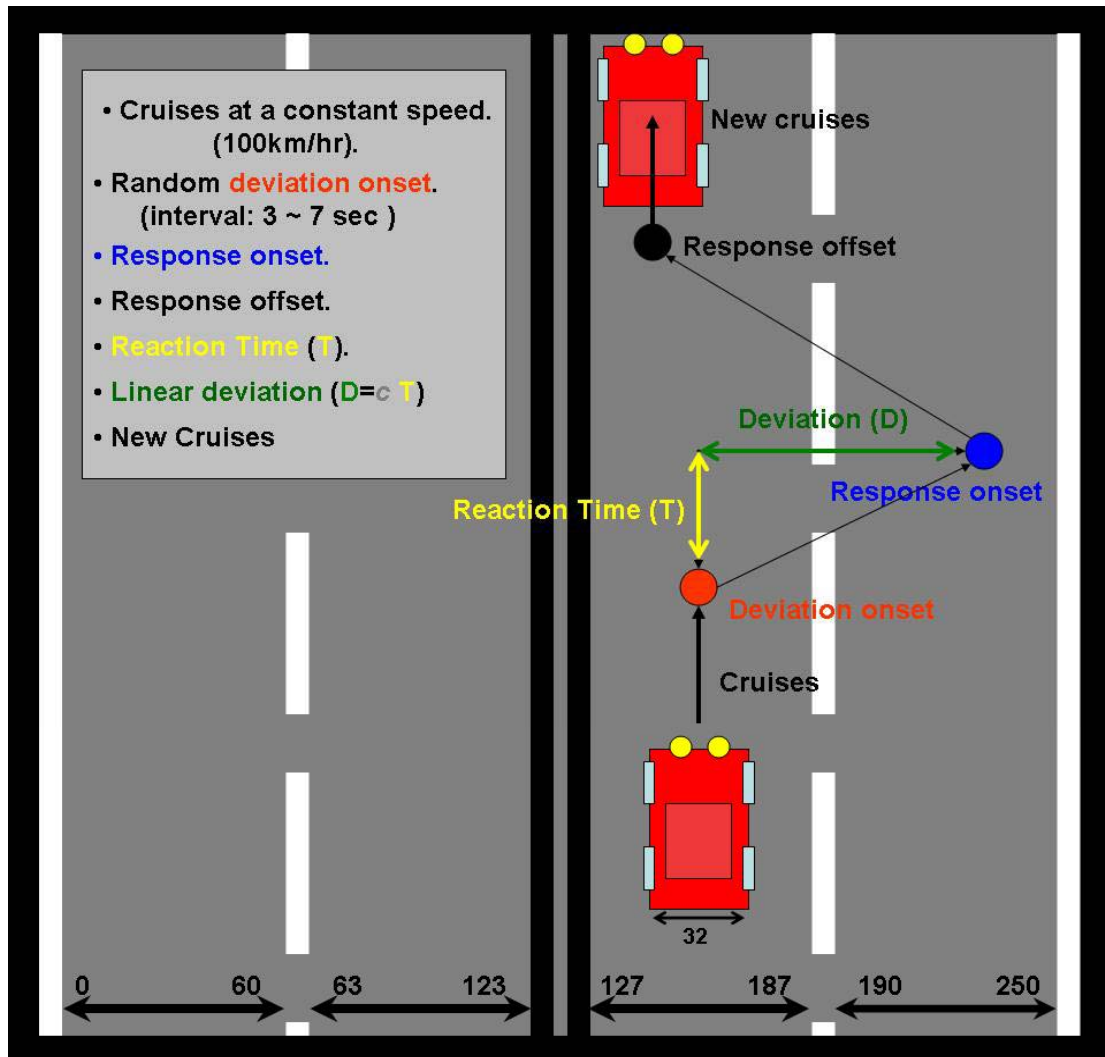


Figure 2. The digitized highway scene. The width of highway is equally divided into 256 units and the width of the car is 32 units. An example of the deviation event. The car cruised with a fixed velocity of 100 km/hr on the VR-based highway scene and it was randomly drifted either to the left or to the right away from the cruising position with a constant velocity. The subjects were instructed to steer the vehicle back to the center of the cruising lane as quickly as possible.

2.2 The EEG data collection

The data acquisition system uses 32 sintered Ag/AgCl EEG/EOG electrodes with a unipolar reference at right earlobe and 2 ECG channels in bipolar connection which are placed on the chest. All EEG/EOG electrodes were placed following a modified International 10–20 system and refer to right ear lobe as depicted in Figure 3. We use the following notations: F: Frontal lobe. T: Temporal lobe. C: Central lobe. P: Parietal lobe. O: Occipital lobe. "Z" refers to an electrode placed on the mid-line. In this figure, A1 and A2 are two reference channels. The two channels FP1 and FP2 are found to be quite noisy and hence we do not use the signals obtained from them. Thus we use data from 28 channels. Before the data acquisition, the contact impedance between EEG electrodes and cortex was calibrated to be less than 5 k Ω . We use the Scan NuAmps Express system (Compumedics Ltd., VIC, Australia) to simultaneously record the EEG/EOG data and the deviation between the center of the vehicle and the center of the cruising lane. The EEG data are recorded with 16-bit quantization level at the sampling rate of 500 Hz. To reduce the burden of computation, the data are then down-sampled to sampling rate of 250 Hz. Since the objective is to develop methodologies that can be used in real time, we do not use sophisticated noise cleaning techniques such as ICA but we preprocess the EEG signals using a simple low-pass filter with a cutoff frequency of 50 Hz to remove the line noise (60 Hz and

its harmonics) and other high-frequency noise.

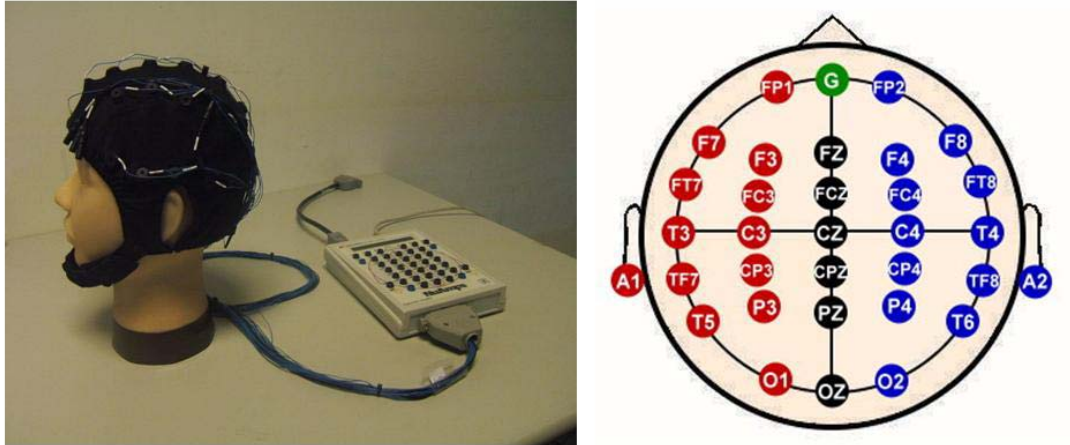


Figure 3. The 32 channel EEG cap and electrodes placement of international 10–20 system. The letters used are: F: Frontal lobe. T: Temporal lobe. C: Central lobe. P: Parietal lobe. O: Occipital lobe. "Z" refers to an electrode placed on the mid-line.

2.3 Subjects

Here we provide a brief description of the EEG recording system as well as of the subjects involved in this study. We have used a set of thirteen subjects (ages varying from 20 to 40 years old) to generate data for the investigation. Of this thirteen, ten subjects are the same as used in [28]. Statistical reports [31] suggest that people often get drowsy within one hour of continuous driving in the early afternoon hours. Moreover, after a good sleep in the night, people are not likely to fall sleep easily during the first half of the day. And hence, we have conducted all our experiments in the early afternoon after lunch so that we can generate more useful data. We have

explained the participants about the goal of these experiments and the general features of the driving task. We have also completed the necessary formalities to get their consent for these experiments. Each subject was asked to drive the car for 60-minutes with a view to keeping the car at the center of the cruising lane by maneuvering it with the steering wheel. Of the thirteen subjects, four struggled with mild drowsiness, while the remaining nine exhibited mild and deep drowsy episodes during the 1-hour driving session.

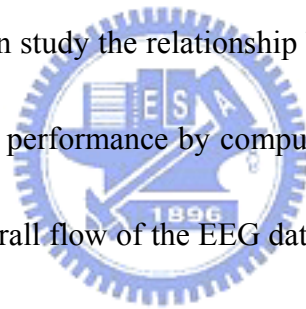


Chapter 3

The unsupervised approach

It is recognized that the changes in EEG spectra in the theta band (4~7Hz) and alpha band (8~11Hz) reflect changes in the cognitive and memory performance [32]. Other studies have reported that EEG power spectra at the theta band [33, 34] and/or alpha band [35, 36] are associated with drowsiness, and EEG log power and subject's driving performance are largely linearly related. These findings have motivated us to derive the alert models of the driver using the alpha-band and theta-band EEG power spectrum computed using Oz channel output recorded in the first few minutes of driving. The choice of the Oz channel is explained in the Experimental Results section. We emphasize that the few minutes of data used to find the alert model are not necessarily collected from the very beginning of driving session because different factors, such as walking of driver by a few meters to reach the garage, may influence the EEG signal generated at the very beginning. The specific window to be used for generation of the alert model is selected by Mardia test (explained later) [37]. We assume that if the subject/driver is in an alert state, then the EEG power spectra relating to theta band (as well as that relating to alpha band) would follow a multivariate normal distribution. The parameters of the multivariate normal distributions characterize the models. Using the alpha-band and theta-band EEG

power, we identify two normal-distribution based models. Then, we assess the deviation of the current state of the subject from the alert model using Mahalanobis distance (MD). We assume that when the subject continues to remain alert, his/her EEG power should resemble the sample data used to generate the model and hence would match the alert model or template. If the subject becomes drowsy, then its power spectra in the alpha band (and also in theta band) will deviate from the respective model and hence MD will increase. With a view to reducing the effect of spurious noise, MDs are smoothed over a 90-sec moving windows, the window is moved by 2-sec steps. We then study the relationship between smoothed Mahalanobis distance and subject's driving performance by computing the correlation between the two. Figure 4 shows the overall flow of the EEG data analysis. In Figure 4, note that, after the models are identified, the preprocessed alpha band and theta band power data directly go to the blocks for computation of MDA and MDT, respectively. MDT and MDA are measure of deviations of the subject's present state from the respective models, this will be clarified later. The block for computation of MDC makes a linear combination of MDT and MDA. Finally, all three, MDA, MDT and MDC are used in correlation analysis with the driver's performance.



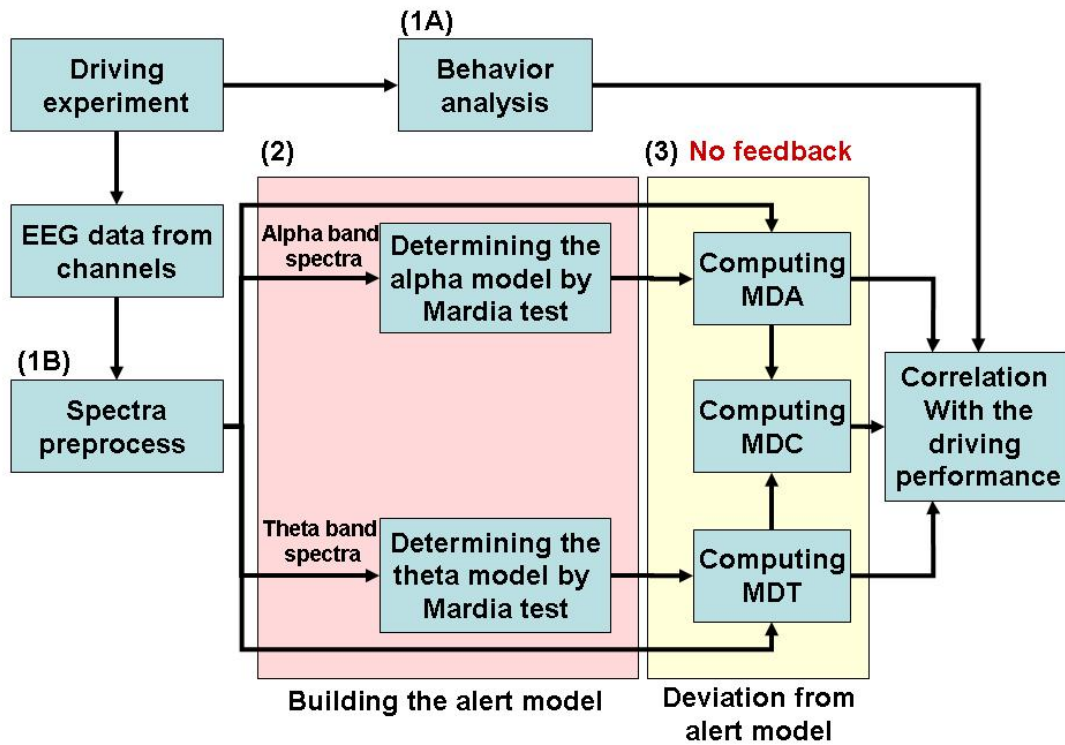
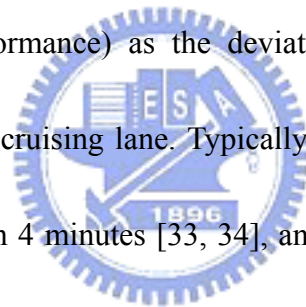


Figure 4. The flowchart of the EEG analysis method. That Contains behavior analysis and EEG analysis. We select theta and alpha-band power while the subject is alert to build two alert models. After the models are build, alpha and theta band power are used to compute deviaions (MD*) from the models. We smooth the resultant MD* with a 90-sec moving window at 2-sec steps and calculate the correlation between subject's driving performance and the smoothed MD*.

3.1 Indirect measurement of alertness

To investigate the relationship between the measured EEG signals and subject's cognitive state, and to quantify the level of the subject's alertness in our previous studies [38-40]. First, we need to quantify the volunteer's drowsiness level in this experiment. When subjects fall drowsy, they often exhibit relative inattention to environments, eye closure, less mobility, failure to motor control and making decision.

Hence, the vehicle deviations were defined as the subject's drowsiness index. The VR-based four-lane straight highway scene was applied in the experiment. In this scene, the four lanes from left to right are separated by a median stripe and the distance from the left side to the right side of the road was equally divided into 256 points indicating the position of the vehicle as the digital output signal of the VR scene at each time instant. The width of each lane and the car is 60 units and 32 units, respectively. Figure 2 shows an example of the driving performance represented by the vehicle deviation trajectories. We have defined an indirect index of the subject's alertness level (driving performance) as the deviation between the center of the vehicle and the center of the cruising lane. Typically the drowsiness level fluctuates with cycle lengths longer than 4 minutes [33, 34], and hence we smooth the indirect alertness level index using a causal 90-sec moving window advancing at 2-sec steps. This helps us to eliminate variance with cycle lengths shorter than 1-2 minutes. We emphasize that this index is used only to validate our approach, and it is not as an input to develop the model for the alert state of the subject. Figure 5 shows the processes of driving performance analysis as precedence.



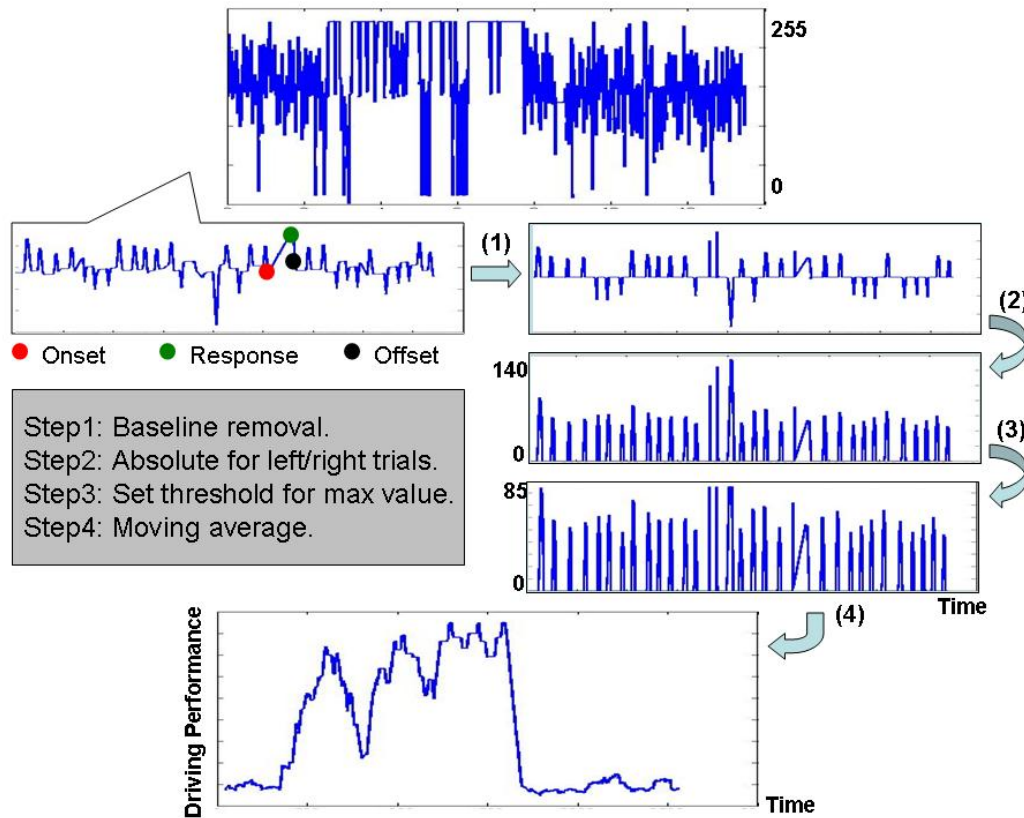


Figure 5. The process of driving performance . Step1: Finding the baseline (deviation onset), and remove it . Step2: Computing the absolute value for the same direction. Step3: Setting the threshold to correct value. Step4: Moving average.

3.2 Smoothing of the Power Spectra.

We use a component-wise median filter for smoothing the power spectrum data. We compute one data vector (a vector with power spectrum) in 20 dimensions using 2 seconds signal using FFT. Thus, we consider 500-point Hanning windows *without* overlap. Each windowed 500-point epoch is now sub-divided into 16 sub-epochs each with 125 points using a Hanning window. Each sub-epoch is shifted by 25-points. For example, the first sub-epoch uses points 1 through 125, the second sub-epoch uses points 26 through 150 and so on. Each sub-epoch is then extended to 256 points by

zero padding for a 256-point FFT. A moving median (computed using the 16 sub-epochs) filter is used to minimize the presence of artifacts in the EEG records of all sub-windows. The median filter is realized by computing the median of each component. In other words, for 2 seconds signal, we have generated 16 vectors, each in 20 dimensions. Then we generate a new vector in 20 dimensions, where the i th component is the median value of the i th component of the 16 vectors. This new vector we call the *moving median filtered* data. This process is repeated for every two seconds without overlap. The moving- median filtered EEG power spectra are then converted to a logarithmic scale prior to further analysis. Logarithmic scaling linearizes the expected multiplicative effects of sub-cortical systems involved in wake-sleep regulation on EEG amplitudes [42]. Thus, for each session EEG log power time series at alpha band as well as at theta band with 2s (500-point, an epoch) time intervals are generated. These time series data are the inputs to our model. Figure 6 shows the processes of spectra analysis as precedence.

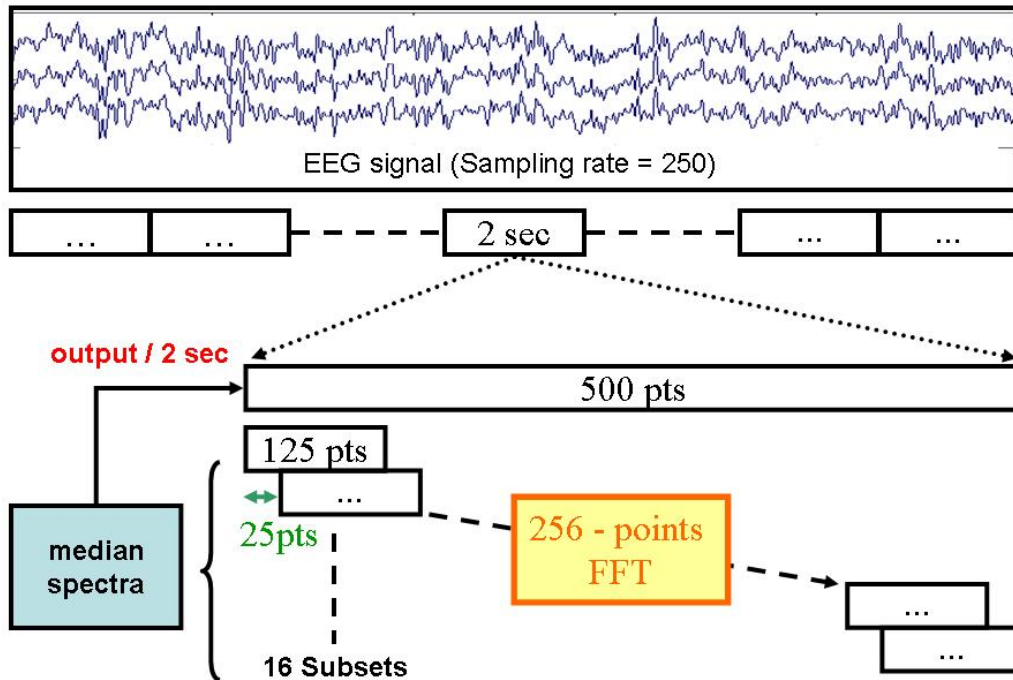


Figure 6. The EEG power spectral analysis procedure. The raw EEG data first accomplished using a 500-point Hanning window without overlap. Windowed 500-point epochs were further subdivided into several 125-point subwindows using the Hanning window again with 25-point step. Each 125-point frame was extended to 256 points by zero-padding to calculate its power spectrum by using a 256-point fast Fourier transform (FFT), resulting in power-spectrum density estimation with a frequency resolution near 1 Hz.

3.3 Computation of the alert model of the subject

In our approach for every subject in every driving session a new model will be constructed. Consequently the variability between subjects as well as the inter-session variability is no more important; these are taken into account automatically. To develop the alert model we make a few mild but realistic assumptions as follows:

1. *The subject is usually very alert immediately after he/she starts the driving session.*
2. *Subject's cognitive state can be characterized by the power spectrum of his/her EEG*
3. *When the person is in the alert state, it can be modeled reasonably well using a multivariate distribution of the power spectrum.*
4. *The alert model expresses well the EEG spectra when the subject remains alert or return to alert state from drowsiness.*



One can argue that the subject may already be in a drowsy state when he/she begins driving. If that is really true, then that can be detected by checking the consistency between two alert models derived using data in two successive time intervals. In other words, we can check whether the two alert-models identifies in two successive time intervals are statistically same or not. If the subject was already in a drowsy state, then he/she will either move to a deep drowsy/sleepy state or will transit to an alert state. In both cases, the two models will not be statistically the same.

Here we use a multivariate distribution to model the distribution of power spectrum in the alert state. In particular, at every 2 second, we calculate the power spectrum vector in p dimension (in our experiment $p = 4$ (theta band) or $p=5$ (alpha band)). In this way, a set of $n=30$ data vectors $\{\mathbf{x}_1, \dots, \mathbf{x}_{30}\}$ is generated in every minute. We use 3 minutes of spectral data to derive the alert model. The alert model is represented and characterized by a multivariate normal distribution $N(\mu, \Sigma^2)$, where μ is the mean vector and Σ is the variance-covariance matrix.

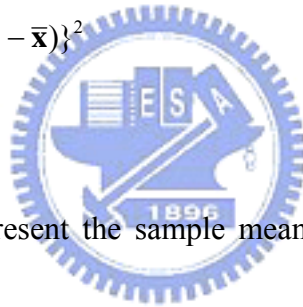
We use the maximum likelihood estimates for μ and Σ^2 . After finding the alert model we check whether the EEG spectrum in the alpha band (also in theta band) indeed follows a multivariate normal using Mardia's test [43-44]. If the model passes the Mardia's test, we accept that model as the alert model. Otherwise, we move the data window by one minute and again use the next 3 minutes of data to derive and validate the model using Mardia's test. Once a model is built, a significant deviation from the model can be taken as a departure from alertness. Note that, we are saying "departure from alertness" which is not necessarily drowsiness. For example, the subject could be excited over a continued conversation over a mobile phone. In this case, although the person is not drowsy, he/she is not alert as far as the driving task is concerned and hence needs to be cautioned. Thus our approach is more useful than

typical drowsiness detection systems. A consistent and significant deviation for some time can be taken as an indicator of drowsiness.

For the sake of completeness, we briefly explain the Mardia's test of multi-variate normality. Given a random sample, $X=\{\mathbf{x}_1,\dots,\mathbf{x}_n\}$ in \mathbb{R}^p , Mardia [43-44] defined the p-variate skewness and kurtosis as:

$$b_{1,p} = \frac{1}{n^2} \sum_{i=1}^n \sum_{j=1}^n \{(\mathbf{x}_i - \bar{\mathbf{x}})'S^{-1}(\mathbf{x}_j - \bar{\mathbf{x}})\}^3 \quad (1)$$

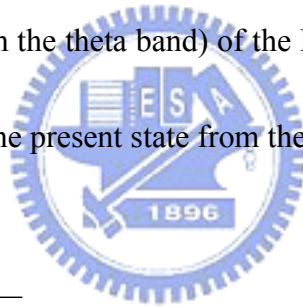
$$b_{2,p} = \frac{1}{n} \sum_{i=1}^n (\mathbf{x}_i - \bar{\mathbf{x}})'S^{-1}(\mathbf{x}_i - \bar{\mathbf{x}})\}^2 \quad (2)$$



In (1) and (2) $\bar{\mathbf{x}}$ and S represent the sample mean vector and covariance matrix, respectively. In the case of university data, $b_{1,p}$ and $b_{2,p}$ reduces to the usual university measures skewness and kurtosis, respectively. If the sample is obtained from a multivariate normal distribution, then the limiting distribution of $b_{1,p}$ is a Chi-square with $p(p + 1)(p + 2)/6$ degrees of freedom, while that of $\sqrt{n}(b_{2,p} - p(p + 2))/8\sqrt{p(p + 2)}$ is $N(0,1)$. Hence we can use these statistics to test multi-variate normality. In all our experiments, we have used the routines available for Mardia's test in the R-package [45].

3.4 Computation of the deviation from the Subject

After the alert model is found, we use it to assess the subject's cognitive state. This was done by finding how the subject's present state, as represented by the EEG power spectra, and was different from the state represented by the alert model. The deviation of the present state from the model is computed using Mahalanobis distance [46] that can account for the covariance between variables while computing the distance. Let the alert model computed using the alpha band be represented by $(\bar{\mathbf{x}}, S)_A$ and that by the theta band be represented by $(\bar{\mathbf{x}}, S)_T$. Let \mathbf{x} be a vector representing the power spectra in the alpha band (or in the theta band) of the EEG of the subject at some time instant, then the deviation of the present state from the model is:



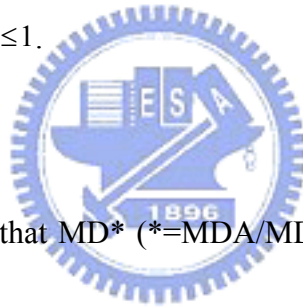
$$MD^*(\mathbf{x}) = \sqrt{(\mathbf{x} - \bar{\mathbf{x}})^T S^{-1} (\mathbf{x} - \bar{\mathbf{x}})} \quad (3)$$

In (3) if we use the alpha band model, then * is A, and for the theta band model and data, * will be T. Thus the deviation from the alpha band model will be denoted by MDA and that for the theta band model will be denoted by MDT. Similar to the pre-processing of the indirect alertness level index (driving performance), the MDA/MDT is also smoothed by the moving average method using a window with a window of 90 seconds. The moving average window is shifted by just one value (i.e.,

2 sec). For a better visual display, we have scaled the MD^* values by subtracting the average MD^* computed over the training data used for finding the alert model.

We shall see later that the deviation from either the alpha band model (i.e., MDA) or the theta band model (i.e., MDT) can be used to detect departure from the alert cognitive state. This raises a natural question, can a combined use of MDA and MDT do a better job than individual ones. To explore such a possibility we use a linear combination MDA and MDT to compute a combined measure of deviation as

$$MDC = a.MDA + (1-a).MDT, 0 \leq a \leq 1.$$



Now in order to demonstrate that MD^* ($=MDA/MDT/MDC$) can be used to detect changes in the cognitive states, we compute the linear correlation between the alertness level index (d) and the smoothed Mahalanobis distance (MD^*). In our subsequent discussion MD^* will represent the smoothed deviations; i.e., the smoothed value of MDA, MDT and MDC as the case may be. The correlation coefficient is defined as:

$$Corr_{d,MD^*} = \frac{\sum (d - \bar{d})(MD^* - \overline{MD^*})}{\sqrt{\sum (d - \bar{d})^2} \sqrt{\sum (MD^* - \overline{MD^*})^2}} \quad (4)$$

3.5 Sorted driving performance spectral analysis

Since the driving performance is an indirect index of the alertness level, we propose the sorted analysis method that sorts the smoothed log power spectra and MD* according to the driving performance index to assess the brain dynamics corresponding to the transition from alertness (lower driving performance values) to drowsiness (larger driving performance values) in driving. This process is used to observe the features change as the increase of driving performance index.



Chapter 4

Results

There are a few important issues to be resolved before we can proceed with the detailed analysis. The first issue is the optimal window size for feature extraction (computing FFT). For this we have tried various choices and have found that 2 sec signal does a reasonably good job and that is what we use here. Note that, one can use a more systematic approach using training and validation data to find the optimal window size. Figure 7 shows the example of MDA/MDT and their correlation with driving performance.



4.1 The choice of channels

The next issue is the choice of channels to be used for analysis. We have data from 28 EEG channels and we wanted to use only one channel to minimize computational complexity. To find the most useful channel for the problem at hand, for each channel we compute the average correlation (averaged over all subjects) between MDA and the driving performance. Similarly, we also compute the average correlation between MDT and the driving performance. These correlation values are summarized in Table 1. Table 1 reveals that, the highest correlation occurs for Channel Oz both with MDT and MDA. This suggests that the channel Oz is better than other channels in

discriminating departure from alertness. The channels O1 and O2 which are neighbors of Oz also exhibit very high correlations. Since we have decided to use only one channel, we have chosen channel Oz for further study.

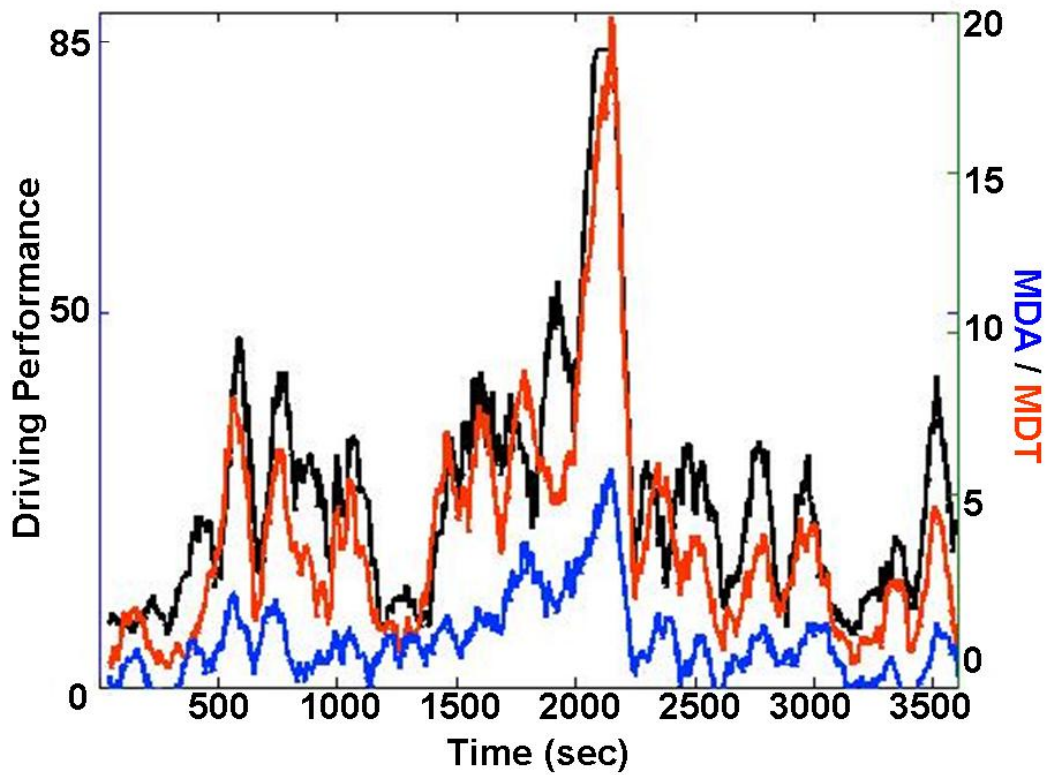


Figure 7. Example of MDA, MDT, and driving performance. After finding the MDT and MDA, we compute their correlations with driving performance.

TABLE 1
THE AVERAGE CORRELATION BETWEEN MAHALANOBIS DISTANCE AND DRIVING
PERFORMANCE OF ALL SUBJECTS FOR DIFFERENT CHANNELS

Pole	F7	F3	FZ	F4	F8	FT7	FC3	FCZ	FC4	FT8
MDA	0.52	0.45	0.59	0.47	0.47	0.53	0.59	0.60	0.56	0.48
MDT	0.13	0.25	0.42	0.23	0.09	0.27	0.56	0.60	0.46	0.13
Pole	T3	C3	CZ	C4	T4	TP7	CP3	CPZ	CP4	TP8
MDA	0.60	0.58	0.58	0.54	0.48	0.54	0.57	0.57	0.51	0.52
MDT	0.38	0.60	0.63	0.54	0.34	0.53	0.58	0.67	0.55	0.53
Pole	P7	P3	PZ	P4	P8	O1	Oz	O2	--	--
MDA	0.56	0.56	0.52	0.53	0.53	0.60	0.64	0.64	--	--
MDT	0.57	0.64	0.66	0.63	0.65	0.71	0.74	0.73	--	--

4.2 Performance sorted analysis

To investigate the relationship between the driver's performance and the concurrent changes in the EEG spectrum, we have sorted the EEG power spectra in alpha band by smoothed driving performance. The similar sorting is also done for power in the theta band. Figure 8(A) depicts the relation between the alpha power and the driving performance, while Figure 8(B) displays the same for theta power. Figure 8(A) reveals that when the driving performance increases from 0 to 20, the mean of alpha (8~12Hz) power rises sharply and monotonically from 19 to 21dB, after that it slowly goes down a little bit. While for the Theta (4~7Hz) power (Figure 8(B)), the mean power increases monotonically and steadily from 20 to 23 dB as the driving performance increases (alertness to deep drowsiness).

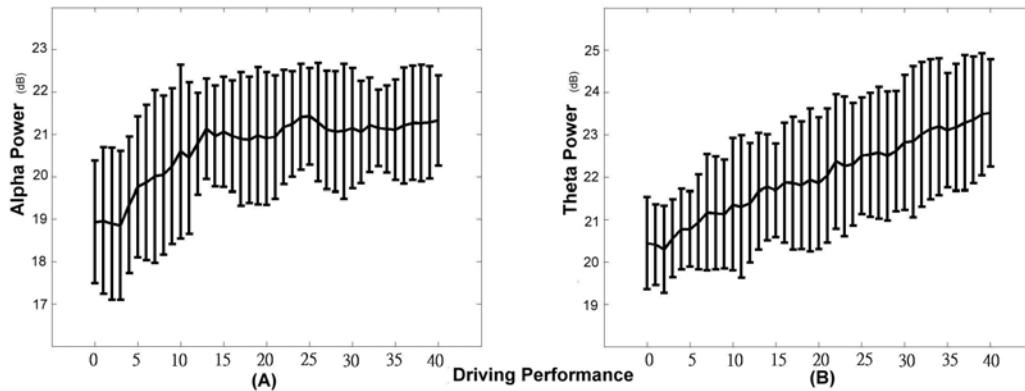
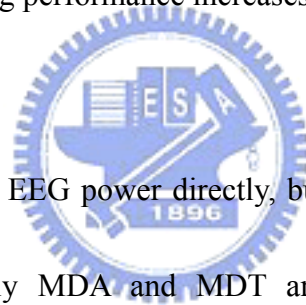


Figure 8. Performance-sorted EEG spectra at Oz over 13 sessions. (A) The solid lines represent the grand mean power spectra and the dotted lines represent the standard deviations of the power spectra. When the driving performance increases from 0 to 20, the mean of alpha power (8~12Hz) rises sharply and monotonically from 19 to 21dB, after which it remains more or less stable near 2 dB above the baseline. (B) The mean of theta power (4~7Hz) increases monotonically and steadily from 20 to 23 dB as the driving performance increases (alertness to deep drowsiness).



Our alert model does not use EEG power directly, but putative MDT and MDA. So next we check how strongly MDA and MDT are correlated with the driving performance. Figure 9(A) shows the relation between driving performance and MDA (across the 13 test subjects/sessions) while Figure 9(B) exhibit the same for MDT. It is interesting to see that, Figure 8 and Figure 9 exhibit almost the same behavior; in fact, for Figure 9(B) we find that compared to Figure 8(B), the average MDT increases more steadily with driving performance.

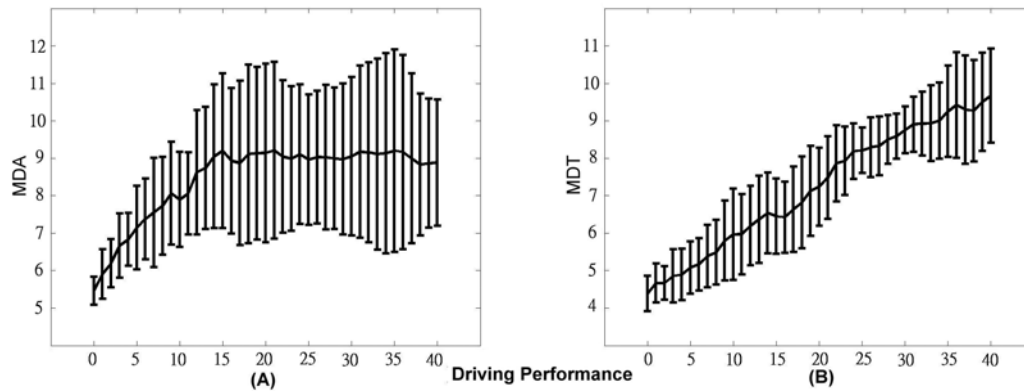
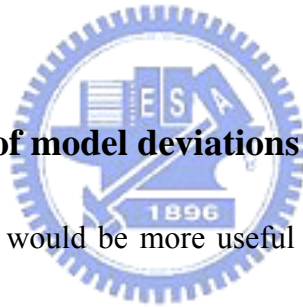


Figure 9. Performance-sorted MD for different sessions. (A) The solid lines represent the grand mean MD and the dotted lines represent its standard deviations. When the driving performance increases from 0 to 20, the MDA rises sharply and monotonically from 5 to 9, after which it remains more or less stable. (B) The MDT increases monotonically and steadily from 4 to 9 as the driving performance increases (alertness to deep drowsiness).

4.3 Linear combination of model deviations



Can we say that use of MD* would be more useful than the use of alpha and theta power? To address this question, for every subject we have computed the correlation between EEG power (in alpha and theta bands) and driving performance and also the correlation between MD* (MDA and MDT) and driving performance. Table 2 summarizes the correlation values. Table 2 reveals that of the 26 sets of correlation values, in 16 cases the correlation has increased with MD*. In a few cases, the increase in correlation is very high. For example, with subject S8, the correlation with alpha power is only 0.04 while that with MDA is 0.76. Similarly, for S6, the alpha power correlation is 0.26 which enhances to 0.63 for MDA. This clearly indicates the

effectiveness of the alert model. Table 2 also displays the average correlation values.

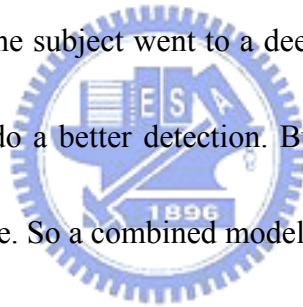
The average correlation with deviations from the model is increased by about 30% for alpha band while that for the theta band is increased by about 23%.

TABLE 2
THE COMPARISON OF THE CORRELATION BETWEEN POWER AND DRIVING PERFORMANCE
AND MD* AND DRIVING PERFORMANCE FOR CHANNEL OZ

drowsiness experiments	Power Correlation (alpha / theta)	Distance Correlation (MDA/MDT)
S1	0.57 / 0.34	0.75 / 0.73
S2	0.70 / 0.51	0.69 / 0.47
S3	0.63 / 0.60	0.67 / 0.65
S4	0.26 / 0.14	0.47 / 0.41
S5	0.66 / 0.79	0.62 / 0.85
S6	0.26 / 0.88	0.63 / 0.85
S7	0.66 / 0.97	0.57 / 0.96
S8	0.04 / 0.72	0.76 / 0.80
S9	0.41 / 0.78	0.39 / 0.77
S10	0.60 / 0.87	0.76 / 0.88
S11	0.40 / 0.57	0.53 / 0.90
S12	0.35 / 0.52	0.24 / 0.62
S13	0.40 / 0.94	0.45 / 0.95
Average	0.45 / 0.62	0.58 / 0.76

The analysis above provides strong and convincing evidence that changes in driving performance during a long driving session is related to the changes in the EEG power in the alpha and theta bands. In the given experimental set up, higher driving performance corresponds to departure from alert state of mind. Thus, departures from

alert cognitive state are reflected in the EEG power of the alpha and theta band. The change (correlation) is more strongly visible in the deviations from the alert model derived based on multivariate normal distribution. We have experimented with two models, one based on alpha band and other based on the theta band. Both appear quite effective. But can we improve it further using the two bands/models together? Figure 10 displays the MDT and MDA as a function of driving performance. From these figures as well as from Table 2, we find that driving performance of mild drowsy cases are more strongly related to MDA while MDT is highly correlated with driving performance for cases when the subject went to a deep drowsy state. Thus, if we can use the right model, we can do a better detection. But in reality, we shall not know beforehand which model to use. So a combined model could be more useful.



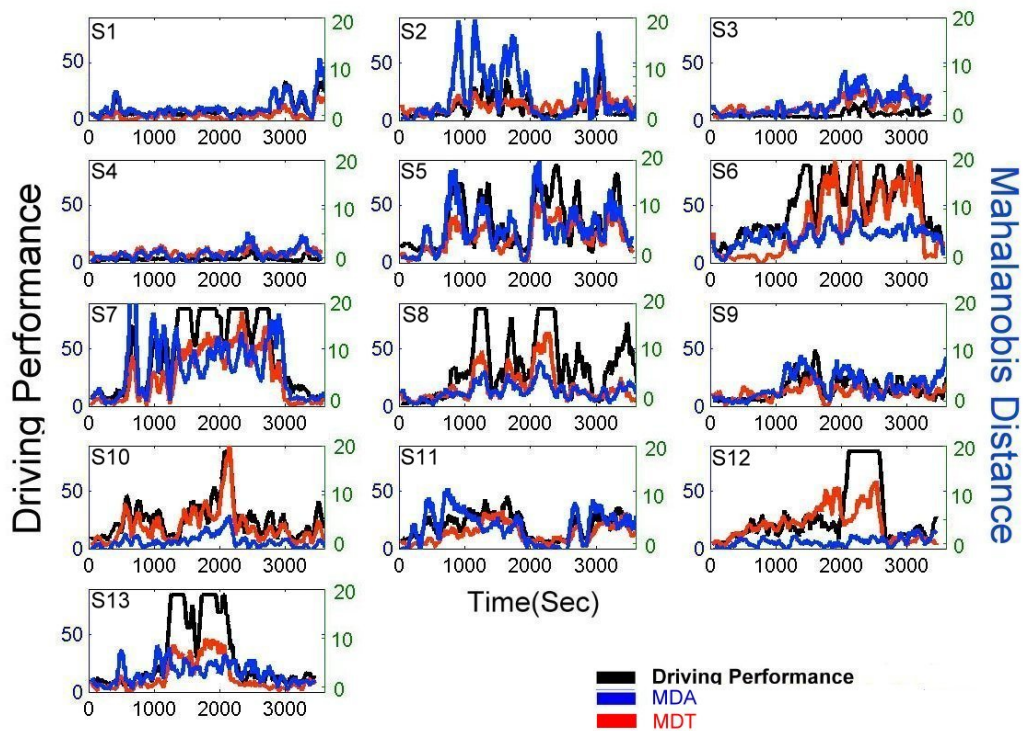


Figure 10. MDT and MDA vs. actual driving performance. Some subject such as S1 has experienced mild drowsiness and MDA is strongly correlated with subject's driving performance. Another subject, S10, was in a deep drowsy state and for this subject MDT is highly correlated with his driving performance.

To examine this possibility, we consider a very simple liner combination of MDA and MDT as $MDC = a.MDA + (1-a).MDT, 0 \leq a \leq 1$. There are infinitely possible choices for the constant a in the linear combination. We have used a grid search starting from $a = 0$ to $a=1$ with an increment of 0.1 and for every such linear combination we have computed the correlation of MDC with driving performance. Based on the limited data set that we have used, we found $a = 0.3$ as the best choice. Table 3 lists the correlation values for a few illustrative cases. Note that, in the second column we

have two correlation values x/y where x corresponds to MDA (i.e., $a = 1$) and y corresponds to MDT (i.e. $a=0$). Table3, in its last row, displays the average correlation values. Although the improvement in average correlation is marginal, what is important is that for the combined model for both deep drowsy and mild drowsy cases we get a very good correlation. As an example, for subject S9, if we use MDA, the correlation is only 0.39, while using MDC, for all combinations the correlation is higher than that with MDA. This justifies the utility of the combined model. Figure 11 depicts the driving performance and the MDC for all 13 subjects. It is clear from these figures that on average, MDC is in more agreement with the driving performance.



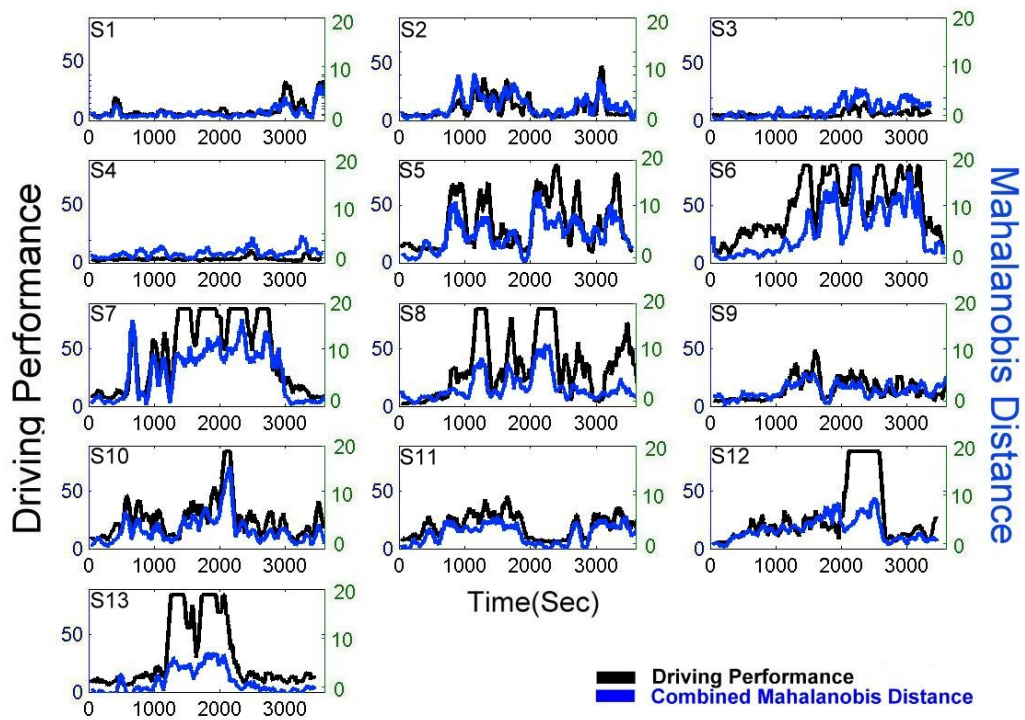


Figure 11. The time series of MDC ($0.3\text{MDA} + .07\text{MDT}$) from Oz channel and the driving performance of all subjects. The black line represents driving performance and the blue line corresponds to MDC. The MDC is found to be highly correlated with driving performance.

TABLE 3

THE CORRELATION VALUES BETWEEN DIRIVING PERFORMANCE AND MDC FOR VARIOUS COMBINATIONS OF MDA AND MDT OVER ALL SUBJECTS USING OZ CHANNEL

drowsiness experiments	Correlation (MDA / MDT)	Correlation 0.1* MDA 0.9* MDT	Correlation 0.3* MDA 0.7* MDT	Correlation 0.5* MDA 0.5* MDT	Correlation 0.7* MDA 0.3* MDT	Correlation 0.9* MDA 0.1* MDT
S1	0.75 / 0.73	0.75	0.78	0.77	0.77	0.75
S2	0.69 / 0.47	0.59	0.67	0.69	0.69	0.69
S3	0.67 / 0.65	0.66	0.68	0.69	0.69	0.68
S4	0.47 / 0.41	0.43	0.46	0.48	0.48	0.47
S5	0.62 / 0.85	0.84	0.80	0.75	0.70	0.65
S6	0.63 / 0.85	0.86	0.86	0.85	0.83	0.74
S7	0.57 / 0.96	0.95	0.92	0.84	0.74	0.62
S8	0.76 / 0.80	0.80	0.81	0.82	0.81	0.79
S9	0.39 / 0.77	0.77	0.75	0.69	0.58	0.45
S10	0.76 / 0.88	0.88	0.88	0.87	0.85	0.81
S11	0.53 / 0.90	0.92	0.9	0.86	0.74	0.60
S12	0.24 / 0.62	0.64	0.65	0.67	0.65	0.45
S13	0.45 / 0.95	0.95	0.93	0.87	0.75	0.56
Average	0.58 / 0.76	0.77	0.78	0.76	0.71	0.64

Chapter 5

Discussion

In this study, we try to build an alert model to observe subject's stage from alertness to drowsiness depended on subject's driving performance. Thus there are some issues that we are interested.

5.1 Alertness model

We have assumed that when a subject starts driving, he is in an alert state. However, this may not necessarily be true. If the person is not in an alert state (i.e., he /she is in a drowsy state) then either he will move to a deep drowsy state or will get to the alert state with time. Thus his/her EEG power spectrum will change with time. This type of situations can be detected using a consistency check as explained earlier. For example, we can find two alert models of the person at time instant t sec and at $t+\delta$ sec, where δ may be 180 seconds. If the person is in an alert state, then these two models will statistically be the same. So we can use such hypothesis testing to authenticate whether the person is in an alert state at the beginning or not. If desired, this can be further strengthened having a stored alert model. If the consistency check explained above fails, then we can check the similarity between the stored model and the model just found. If these two models are also significantly different, this will

further suggest that the person is not in an alert state at the beginning.

5.2 Feature selection

The data set used in this study is not very big and not balance. Of the 13 subjects four subjects were mild drowsy during the driving experiments, while the remaining subjects went through episodes of mild drowsy to deep drowsy states. To demonstrate the effectiveness of this method, further investigation using a bigger set needs to be done. And, we have used only alpha band and theta band from Oz channel. Use of more signals (like EOG) and different spectra (like beta band) along with alpha band and theta band from Oz might improve the system performance.

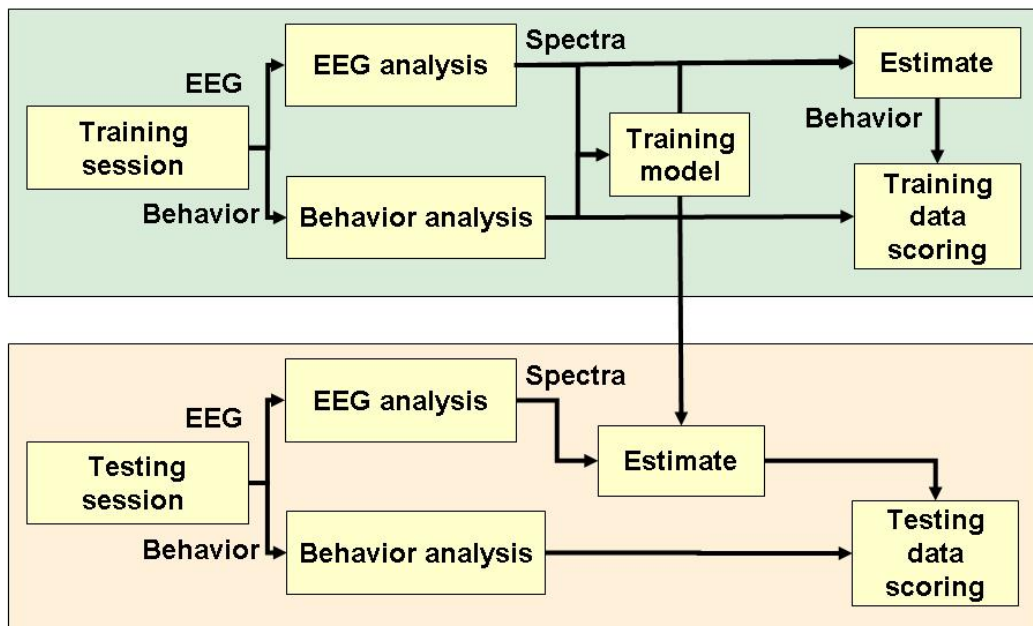


5.3 Supervised and unsupervised

In this study, we use an unsupervised method to observe subject's drowsy cognition. But a supervised method [18], flowchart will like Figure 12. In this figure, we can know several things:

1. *Supervised method needs data (trained before) feedback. So we will always need to take double of cost.*
2. *Supervised method estimate driving performance. So, if some stage we did not learn at training data, we can not estimate it accurately.*

Unsupervised method is good at out of illustrations above. But that is hard to define the output of result. In this paper, we try to find the most useful channels and using the drowsy related features (alpha/theta) to make sure the deviation from alert model is related to drowsiness. And, because of, the output of these two methods are different, we can not compare the performance between these two methods. But depend on correlation with driving performance; we had little lower value than supervised method.



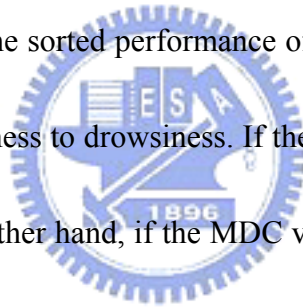
3

Figure 12. The flowchart of supervised method. We need two sessions of experiments to perform this method. Using training experiment to produce model and estimation in testing experiment.

5.4 Threshold from alertness to drowsiness

In this investigation, we have demonstrated the feasibility of an unsupervised subject and session independent approach to detect departure from alertness in driver. And we plan to identify thresholds on MDC which can be used to label the driver's cognitive state as alert/drowsy. In figure13 depend on driving performance we get two values of 17 to warn, and 32 to be dangerous. If car shifts 17 pixels, it maybe lost something of control. And if car shifts 32 pixels, it maybe hit other car on another lane.

Then according to figure14, the sorted performance of MDC, we can get 2 thresholds of 3 and 5 to distinguish alertness to drowsiness. If the MDC value is under than 3 the subject may be alert. On the other hand, if the MDC value is bigger than 5 the subject may be drowsy. Then we plot these two thresholds with MDC of all subjects in figure15.



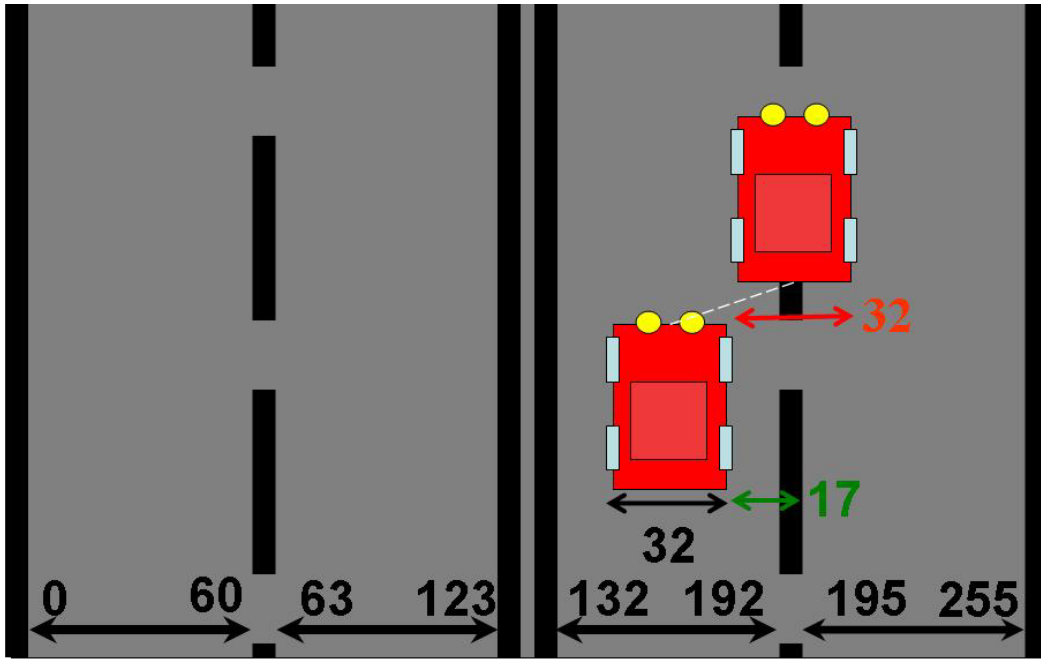
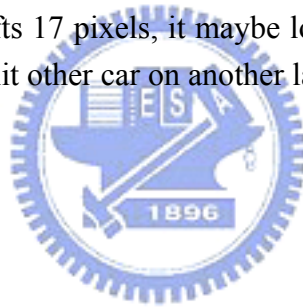


Figure 13. Depend on driving performance we get two values of 17 to warn, and 32 to be dangerous. If car shifts 17 pixels, it maybe lost something of control. And if car shifts 32 pixels, it maybe hit other car on another lane.



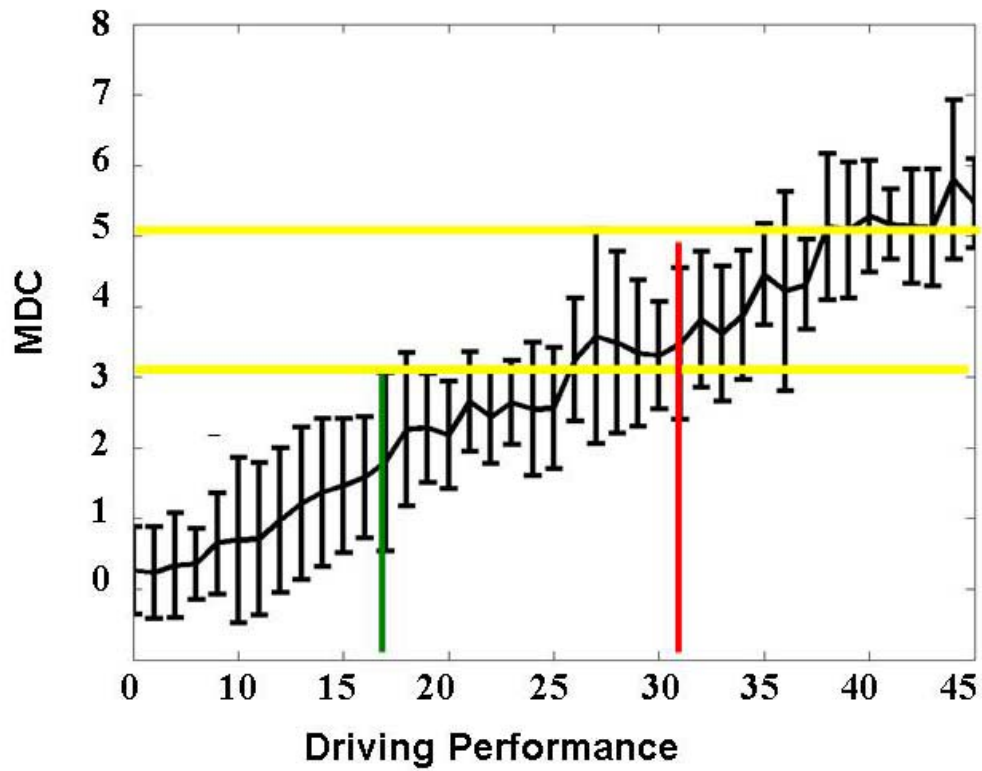


Figure 14. The sorted performance of MDC, we can get 2 thresholds of 3 and 5 to distinguish alertness to drowsiness. If the MDC value is under than 3 the subject may be alert. On the other hand, if the MDC value is bigger than 5 the subject may be drowsy.

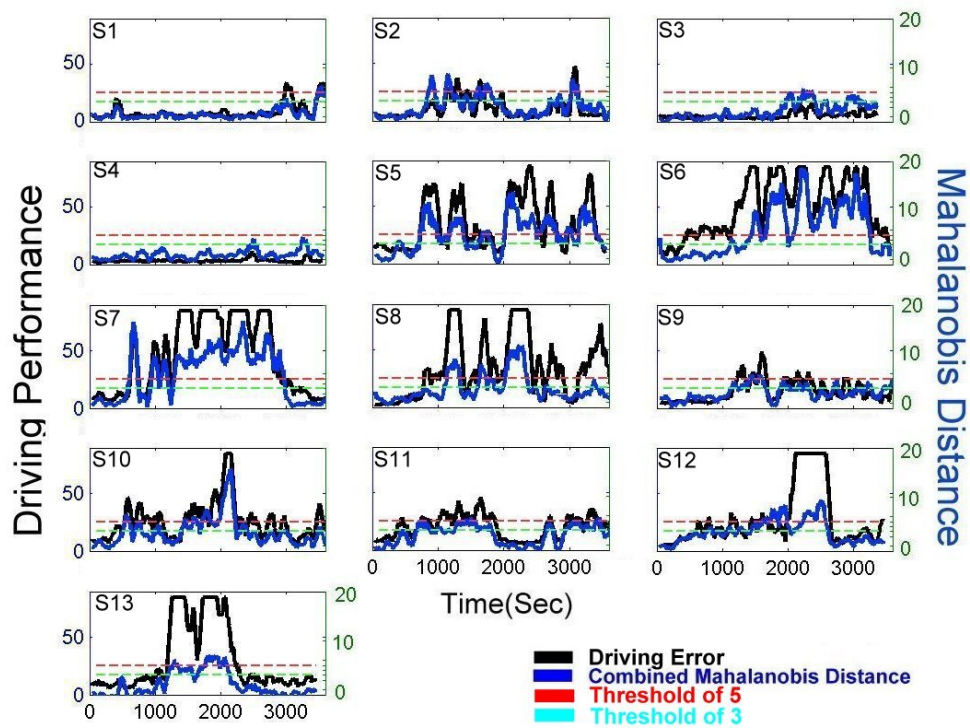


Figure 15. MDC and the threshold from alertness to drowsiness.



5.5 Estimative frequency

In this study, we get the spectra vector every 2 seconds, so the estimative frequency is 2 seconds. It may be dangerous for really case of driving. But, first human's drowsy cognition is gradual change step by step. So, none will change soon from alertness to drowsiness. Otherwise, we can get an overlap from the spectra analysis to make the estimative frequency highly.

Chapter 6

Conclusions

In this study, we propose an unsupervised approach that in every driving session generates a statistical model of the alert state of the subject using a very limited data obtained at the beginning of the driving session. Our model makes a few very realistic assumptions to derive the alert-state model. We assume that the EEG power spectrum in an alert state can be reasonably modeled using a multivariate normal distribution. The model is first validated statistically and then used to assess the cognitive state of the driver. A significant deviation from the model is taken as a departure from the alert state. We also attempt to find good choices of channel(s) and EEG features for assessing the drowsiness-related EEG dynamics. We have found that Oz is an effective channel and the power spectra in the theta band and alpha band have good discriminating power. We have derived three models, one based on alpha band spectrum, one based on the theta band power spectrum and the third one combines the deviations of the subject present cognitive state from the two models. We have demonstrated that deviation of the subject present cognitive state from the alert model co-varies with the driving performance which is an indirect measure of operators' changing levels of alertness when they perform a realistic driving task in a VR-based driving simulator. Unlike most supervised method, our method can account for large

individual and cross-session variability in EEG dynamics.



References

1. K. A. Brookhuis, D. D. Waard, and S. H. Fairclough, "Criteria for driver impairment," *Ergonomics*, Vol 46, 433-445, 2003.
2. URL: <http://www.sleepfoundation.org/>.
3. R. S. Huang, C. J. Kuo, L. L. Tsai, and O. T. C. Chen, "EEG pattern recognition arousal states detection and classification," in *Proc. IEEE Conf. Neural Netw*, vol. 2, pp. 641–646, Jun. 1996.
4. Vuckovic, V. Radivojevic, A. C. N. Chen, and D. Popovic, "Automatic recognition of alertness and drowsiness from EEG by an artificial neural network," in *Med. Eng. Phys*, vol. 24, pp. 349–360, 2002.
5. S. Roberts, I. Rezek, R. Everson, H. Stone, S. Wilson, and C. Alford, "Automated assessment of vigilance using committees of radial basis function analysers," in *Proc. IEEE Sci. Meas. Technol*, vol. 147, pp. 333–338, Nov. 2000.
6. K. B. Khalifa, M. H. Bedoui, R. Raytchev, and M. Dogui, "A portable device for alertness detection," in *Proc. Annual Int. IEEE EMBS Special Topic Conf. Microtechnolog. Med. Biol*, pp. 584–586, Oct. 2000.
7. B. J. Wilson and T. D. Bracewell, "Alertness monitor using neural networks for EEG analysis," in *IEEE Signal Process. Soc. Workshop on Neural Netw. Signal Process*, vol. 2, pp. 814–820, Dec. 2000.
8. K. Van Orden, W. Limbert, S. Makeig, and T. P. Jung, "Eye activity correlates of workload during a visuospatial memory task," *Human Factors*, vol. 43, no. 1, pp. 111–121, 2001.
9. M. Matousek and I. Petersen, "A method for assessing alertness fluctuations from EEG spectra," *Electroencephalogr. Clin. Neurophysiol*, vol. 55, no. 1, pp. 108–113, 1983.

10. J. Beatty, A. Greenberg, W. P. Deibler, and J. O'Hanlon, "Operant control of occipital theta rhythm affects performance, in a radar monitoring task," *Science*, vol. 183, pp. 871–873, 1974.
11. J. A. Stern, D. Boyer, and D. Schroeder, "Blink rate: Possible measure of fatigue," *Human Factors*, vol. 36, pp. 285–297, 1994.
12. D. Schmidt, L. A. Abel, L. F. Dell'Osso, and R. B. Daroff, "Saccade velocity characteristics: Intrinsic variability and fatigue," *Aviation Space Environ. Med.*, vol. 50, pp. 393–395, 1979.
13. D. K. McGregor and J. A. Stern, "Time on task and blink effects on saccade duration," *Ergonomics*, vol. 39, pp. 649–660, 1996.
14. K. Van Orden, T. P. Jung, and S. Makeig, "Combined eye activity measures accurately estimate changes in sustained visual driving performance," *Biol. Psychol*, vol. 52, no. 3, pp. 221–40, 2000.
15. C. Jutten and J. Herault, "Blind separation of sources I. An adaptive algorithm based on neuromimetic architecture," *Signal Process*, vol. 24, pp. 1–10, 1991.
16. P. Comon, "Independent component analysis—A new concept?," *Signal Process*, vol. 36, pp. 287–314, 1994.
17. J. Bell and T. J. Sejnowski, "An information-maximization approach to blind separation and blind deconvolution," *Neural Comput*, vol. 7, pp. 1129–1159, 1995.
18. M. Girolami, "An alternative perspective on adaptive independent component analysis," *Neural Comput*, vol. 10, pp. 2103–2114, 1998.
19. T. W. Lee, M. Girolami, and T. J. Sejnowski, "Independent component analysis using an extended infomax algorithm for mixed sub- and super-Gaussian sources," *Neural Comput*, vol. 11, pp. 606–633, 1999.

20. A. Kemeny, F. Panerai, "Evaluating perception in driving simulation experiments," *TRENDS in Cognitive Sciences*, vol. 7, 1, 2003.
21. W. W. Wierwille, J. G. Casali, B. S. Repa, "Driver steering reaction time to abrupt onset crosswind, as measured in a moving-base driving simulator," *Hum. Factors*, vol. 25, pp. 103-116, 1983.
22. G. Reymond, A. Kemeny, J. Droulez, A. Berthoz, "Role of lateral acceleration in curve driving: driver model and experiments on a real vehicle and a driving simulator," *Hum. Factors*, vol. 43, pp. 483-495, 2001.
23. N. G. Page, M. A. Gresty, "Motorist's vestibular disorientation syndrome. J. Neurol. Neurosurg," *Psychiatry*, vol. 48, pp. 729-735, 1985.
24. E. L. Groen, I. P. Howard, B. S. K. Cheung, "Influence of body roll on visually induced sensation of self-tilt and rotation," *Perception*, vol. 28, pp. 287-297, 1999.
25. J. D. Bayliss, D. H. Ballard, "A Virtual Reality Testbed for Brain-Computer Interface Research," *IEEE Transactions on Rehabilitation Engineering*, vol. 8, pp. 188-190, 2000.
26. H. J. Eoh, M. K. Chung, S. H. Kim, "Electroencephalographic study of drowsiness in simulated driving with sleep deprivation," *International Journal of Industrial Ergonomics*, vol. 35, pp. 307-320, 2005.
27. R. S. Huang, T. P. Jung, Makeig, Scott, "Analyzing Event-Related Brain Dynamics in Continuous Compensatory Tracking Tasks," *IEEE Engineering in Medicine and Biology 27th Annual Conference*, pp. 5750-5753, 2005.
28. Chin-Teng Lin, Nikhil R. Pal, Chien-Yao Chuang, Tzyy-Ping Jung, Li-Wei Ko, Sheng-Fu Liang, "An EEG-based Subject- and Session-independent Drowsiness Detection", *The proceedings of International Joint Conference on Neural*

Networks(IJCNN), World Congress on Computational Intelligence, Hong Kong,
pp. 3448-3454, June 2008.

29. C. T. Lin, R. C. Wu, T. P. Jung, S. F. Liang, and T. Y. Huang, "Estimating alertness level based on EEG spectrum analysis," *EURASIP J. Appl. Signal Process*, vol. no. 19, pp. 3165–3174, Mar. 2005.
30. C. T. Lin, R. C. Wu, S. F. Liang, W. H. Chao, Y. J. Chen, and T. P. Jung, "EEG-based drowsiness estimation for safety driving using independent component analysis," *IEEE Trans on Circuits and Systems*, vol. 52, no. 12, pp. 2726-2738, 2005.
31. H. Ueno, M. Kaneda, and M. Tsukino, "Development of drowsiness detection system," in *Proc. Veh. Navigation Inf. Syst. Conf*, pp. 15–20, Aug. 1994.
32. W. Klimesch, "EEG alpha and theta oscillations reflect cognitive and memory performance: a review and analysis," *Brain Research*, vol 29, pp. 169–195, 1999
33. S. Makeig and T.P. Jung, "Tonic, phasic, and transient EEG correlates of auditory awareness in drowsiness," *Cognitive Brain Research*, vol. 4, pp. 15-25, 1996.
34. S. Makeig, T.P. Jung, and T.J. Sejnowski, "Awareness during drowsiness: dynamics and electrophysiological correlates," *Canadian Journal of Experimental Psychology*, vol., 54, pp.266-273, 2000.
35. M.A, Schier, "Changes in EEG alpha power during simulated driving: a demonstration," *International Journal of Psychophysiology*, vol. 37, pp.155-162, 2000.

36. S.L. Joutsiniemi, S. Kaski, and T. AndreoLarsen, "Self-organizing map in recognition of topographic patterns of EEG spectra," *IEEE Transactions on Biomedical engineering*, Vol. 42, no. 11, 1995.
37. K.V. Mardia, "Mardia's Test of Multinormality," in S. Kotz and N.L. Johnson, eds., *Encyclopedia of Statistical Sciences*, vol. 5, pp. 217-221, 1985
38. S. Makeig and T. P. Jung, "Changes in alertness are a principal component of variance in the EEG spectrum," *NeuroReport*, vol. 7, pp. 213-216, 1995.
39. T. P. Jung, S. Makeig, M. Stensmo, and T. J. Sejnowski, "Estimating alertness from the EEG power spectrum," *IEEE Trans. Biomed. Eng*, vol. 44, no. 1, pp. 60-69, Jan. 1997.
40. S. Makeig and M. Inlow, "Lapses in alertness: Coherence of fluctuations in performance and EEG spectrum," *Electroencephalography. Clin. Neurophysiol*, vol. 86, pp. 23-35, 1993.
41. M. Steriade, "Central core modulation of spontaneous oscillations and sensory transmission in thalamocortical systems," *Current Opinion in Neurobiology*, vol. 3, no. 4, pp. 619-25, 1993.
42. K.V. Mardia. "Measures of multivariate skewness and kurtosis with applications," *Biometrika*, vol.36, pp. 519-530, 1970.
43. K.V. Mardia. "Applications of some measures of multivariate skewness and kurtosis in testing normality and robustness studies," *Sankhyā, Ser B*, vol. 36, no. 2, pp. 115-128, 1974.
44. K.V. Mardia. "Tests of univariate and multivariate normality," In: S. Kotz et al., editors, *Handbook of Statistics*, vol. 1, pp. 279-320, 1980.
45. URL: <http://www.r-project.org/>

46. P.C. Mahalanobis, “generalised distance in statistics,” *Proceedings of the National Institute of Science of India* pp. 49-55, 1936

